

Enhanced Oral Uptake of Tomato Lectin-Conjugated Nanoparticles in the Rat

Nasir Hussain,^{1,2} Praful U. Jani,^{1,3} and Alexander T. Florence^{1,4}

Received January 10, 1997; accepted February 20, 1997

Purpose. To investigate the usefulness of a surface-conjugated, bioadhesive molecule, tomato lectin, to augment intestinal uptake of orally administered inert nanoparticles.

Methods. Fluorescent 500 nm polystyrene nanoparticles with tomato lectin covalently surface coupled using a carbodiimide reaction were administered to female Wistar rats by oral gavage daily for 5 days.

Results. Analysis of tissue extracted polymer by gel permeation chromatography revealed a 23% systemic uptake of tomato lectin conjugated nanoparticles compared to < 0.5% of TL nanoparticles blocked with N-acetylchitotetraose thus representing an increase of almost 50 fold across the intestine. Intestinal uptake of tomato lectin-conjugated nanoparticles via the villous tissue was 15 times higher than uptake by the gut-associated lymphoid tissue.

Conclusions. The application of tomato lectin as a bioadhesive agent *in vivo* has been demonstrated to enhance subsequent intestinal transcytosis of colloidal particulates to which it is bound.

KEY WORDS: tomato lectin; Peyer's patches; nanoparticles; oral uptake; bioadhesion.

INTRODUCTION

The mammalian gastrointestinal tract has been shown to be capable of absorbing and translocating to the blood via the intestinal lymphatics a wide variety of particles ranging from inert matter such as polystyrene nanoparticles (1–4) and carbon particles (5) to live bacteria and viruses (6). While the mechanisms for uptake are not understood completely it is generally accepted that the follicle associated epithelium of the Peyer's patches, particularly the membranous antigen transporting (M-) cells, are the major sites of uptake (7–8). In spite of the accumulated evidence on the translocation of particulate matter there has been no general agreement on the extent of uptake. Recently attention has been focused on exploiting the oral route for absorption of colloidal carriers incorporating non-replicating antigens for oral vaccination and drug molecules that are either susceptible to gastrointestinal degradation or those which are poorly absorbed and which at present can only be administered parenterally. This has obvious advantages for the oral delivery of encapsulated peptide and protein drugs as most, if not all, oral peptide delivery strategies suffer from the inherent disadvantage

that they cannot afford the protection of these drugs beyond the intestinal lumen from cytosolic, interstitial and hepatic degradation. In contrast if useful amounts of polymeric colloidal carriers can be absorbed from the intestine then this offers the systemic bioavailability of encapsulated gastrointestinal labile drugs. Both the extent and reproducibility of intestinal uptake of nanoparticles are crucial for the delivery of peptide and protein drugs which have narrow therapeutic indices. As systemic uptake of colloidal particulates has been found to be low, of the order of 1–2% of the administered oral dose (2), the aim of this study was to explore whether this figure could be increased by the modification of the surface of a carrier with a bioadhesive ligand-specifically tomato lectin (TL).

Here we have further investigated the bioadhesive and endocytic potential of tomato lectin in enhancing 500 nm polystyrene latex particles. Several authors have discussed the possibility of incorporating lectins as a bioadhesive component of a drug delivery system (9–11) but so far no *in vivo* work has been reported (12). Tomato lectin is an appealing candidate due to its apparent lack of toxicity to the intestinal epithelium (13) and its resistance to proteolytic degradation (14).

We report data indicating that up to 23% of tomato lectin-conjugated nanoparticles (500 nm) administered orally to rats for 5 days are translocated into the systemic circulation, representing a 50 fold increase when compared to hapten-blocked nanoparticles which exhibit less than 0.5% systemic absorption.

MATERIALS AND METHODS

Preparation of Tomato Lectin-Nanoparticle Conjugates

Fluorescent carboxylated 500 nm diameter nanoparticles (Polysciences Ltd, Northampton, UK 2.5% w/v) were covalently coupled to tomato lectin (TL) in a similar manner as reported in an earlier report (15). Briefly 4.5 mL of suspension was washed twice in 0.1 M carbonate buffer (pH 9.6) by centrifugation (MSE 50 M centrifuge) at 15000 rpm in 50 mL polycarbonate tubes followed by two washes in 0.1 M phosphate buffer to remove the storage buffer and any adsorbed surfactant or polymeric stabiliser. The nanoparticle pellet was then resuspended by vortexing in 5.5 mL of phosphate buffer to which was added an equal volume of freshly prepared 2% w/v carbodiimide solution (dimethylaminopropyl-3-ethylcarbodiimide HCl, Sigma, UK). The mixture was then shaken gently for 3 h to activate the carboxyl groups, a longer time leading to aggregation. The nanoparticle suspension was then centrifuged to remove the unreacted carbodiimide and further washed twice in 0.1 M borate buffer to remove any traces of carbodiimide which might otherwise cross-link the lectin molecules. To this, 7 mL of borate buffer containing 2 mg of tomato lectin (Vector Laboratories, Peterborough, UK, lyophilised, 60% purity by SDS) was added and the mixture gently shaken overnight at 8°C to allow coupling. 1 mL ethanalamine (0.1 M) was then added to block any remaining specific sites and the mixture shaken for a further 30 min at room temperature. The suspension was then centrifuged and the pellet resuspended in 10 mg/mL BSA solution for 30 min at room temperature to further block any non-specific sites. The nanoparticle suspension was centrifuged as before and resuspended to the original volume (4.5 mL) in distilled water. For controls, tomato lectin-conjugated nanoparticles

¹ Centre for Drug Delivery Research, The School of Pharmacy, University of London, Brunswick Square, London WC1N 1AX, United Kingdom.

² Present Address: Department of Molecular Pharmacology, St. Jude Children's Research Hospital, Memphis, Tennessee 38101.

³ Deceased December 2, 1995.

⁴ To whom correspondence should be addressed. (e-mail: A.T. Florence@ulsop.ac.uk)

were blocked with 10 mg of N-acetylchitotetraose (Sigma, UK), a known potent inhibitor, overnight (14).

Determination of Percentage Coupling of Tomato Lectin to Polystyrene Nanoparticles

A modified Lowrey method (16) was employed to determine the percentage covalent coupling of TL to polystyrene nanoparticles. The method has the advantage of directly determining the amount of protein attached to the nanoparticles as compared to the determination of protein remaining in solution after the incubation of nanoparticles (ie. by difference) which can give inaccurate results. Briefly 200ml of lectin-nanoparticle conjugates were processed as normal protein solution. Upon centrifugation (Biofuge, Germany, 7000 rpm) the resultant supernatant was further clarified by filtration through a 0.2mm filter and the absorbance of the filtrate measured at 750nm. Determination of triplicate readings against a standard BSA calibration curve gave a mean of $60\% \pm 5$ (SD) coupling.

Haemagglutination Test

The retention of activity of the lectin after covalent coupling was assessed by lectin-induced agglutination of human erythrocytes (11). Two-fold serial dilutions of 100mL of the conjugate suspension was made in a microtitre plate. 100mL of a 2%w/v suspension of fresh human blood, washed once with Alsever's (Sigma, Dorset, UK; Citric acid 0.55g/L, Citric acid·3Na·2H₂O 8g/L, NaCl 4.2g/L, glucose 20.5g/L) solution followed by three washes in PBS was then added to each well and incubated at 37°C for 30min. Confirmation of activity was shown by comparing the value of the titre of dilution giving the last visible detectable erythroagglutination against a positive control (TL solution) and two negative controls (uncoated nanoparticles and lectin-conjugated nanoparticles in the presence of N-acetyl tetrachitotetraose [14]). Erythroagglutination is accompanied by the flocculation of erythrocytes, appearing as a diffuse red colour in sharp contrast to the bright red spot in the centre of the well as seen in the case of a negative result due to the sinking of non-agglutinated erythrocytes. The procedure was conducted in triplicate. Titre values for TL-conjugated nanoparticles were one order less than that obtained for tomato lectin test solution thus confirming lectin activity. Both controls, however, exhibited negative results as early as the second dilution.

Oral Administration to Rats

Animals used in the experiments were all maintained, treated and housed according to the guidelines and regulations stipulated by the UK Animals Act 1987. In each experiment a group of 5 female Wistar rats (average weight 180g) were employed, of which 4 were used for quantitation and one for histological examination. Nanoparticles were administered by oral gavage using a blunt-ended feeding needle, a dose of 0.1mL (12.5 mg/Kg) being administered daily for 5 days. Rats were given free access to water but starved overnight before each dose, food being resumed 1h later. A second group of rats were administered an identical dose of TL-conjugated nanoparticles blocked with N-acetylchitotetraose to test for the specificity of epithelial bioadhesion. After the final dose all animals were fasted overnight in a nanoparticle free environment but allowed

water to clear the gut of any unabsorbed nanoparticles. Animals were kept in individual metabolic cages to prevent coprophagia and re-introduction of excreted nanoparticles. Animals were sacrificed using vaporised halothane.

Extraction and Analysis of Polystyrene Nanoparticles from Tissues

Stomach, small intestine, colon, liver, spleen, lungs, kidneys and heart were immediately excised after sacrificing, ensuring no contact with the animal fur. The small intestine was subdivided into lymphoid tissue (Peyer's patches), mesentery nodes and network. Any food or faecal contents present in either the small or large intestine was gently removed by either by longitudinally sectioning the affected region and picking off the contents with forceps followed by gentle washing in PBS or flushing PBS through the intact segments of the intestine, to minimise the possibility of adsorbed nanoparticles being included in the analysis. Scraping was avoided to prevent forcing unabsorbed nanoparticles into the tissues. All tissues prior to extraction were rinsed in PBS, sealed individually in polyethylene bags and frozen immediately in nitrogen and stored frozen at -40°C . In addition 2mL of blood was taken directly through the heart immediately after opening the thoracic cavity and placed in heparin coated vials. Extraction of polystyrene nanoparticles from tissues and subsequent analysis/quantitation by gel permeation chromatography (GPC) (Figure 1) was accomplished by the method of Jani *et al.* (2). At all times steps were taken to prevent cross contamination during extraction and its subsequent analysis on the GPC by routinely washing the columns and injection apparatus after each injection.

Histological Examination

Excised tissue was immediately frozen in Tissue Tek II compound on to a cylindrical chuck using liquid nitrogen and 5mm sections cut at -30°C . Between sectioning the knife was cleaned thoroughly using acetone to prevent cross contamination of nanoparticles between tissues. Nanoparticles were

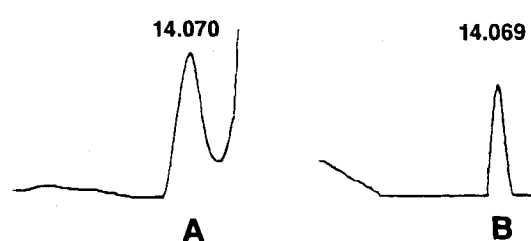


Fig. 1. Typical chromatography peaks obtained after (A) fluorescent nanoparticles (500 nm) dissolved in tetrahydrofuran (THF, Analar grade, Aldrich, UK) for calibration and (B) extraction of tissue sample using chloroform. Peak (B) is that of a blood sample showing the presence of TL-conjugated nanoparticles in the systemic circulation after oral dosing to rats. The percentage recovery of polystyrene from spiked tissue was accomplished by injecting 50mL of the same batch of polystyrene latex used in the production of conjugates into a 25%w/v suspension of homogenised liver. Polystyrene extraction and detection was conducted as described previously (2). A mean value of $80\% \pm 4$ (SD) recovery was obtained from 3 extractions. The lowest limit of polystyrene detection was found to be $2.5 \times 10^{-7}\text{g}$. The retention time of extracted polystyrene remained similar compared to the calibrating test solution of polystyrene in THF as shown above.

observed using a Nikon Microphot FSA microscope with FITC filter.

RESULTS

Tomato-Lectin Induced Intestinal Uptake of Nanoparticles

Quantification of the intestinal uptake of polystyrene nanoparticles on to which tomato lectin was covalently bound was accomplished by GPC. Comparison of the absorption of TL-conjugated nanoparticles with those inhibited with N-acetylchitotetraose (blocked nanoparticles) revealed a 13 fold increase in adsorption/absorption from the intestinal epithelium (Table 1). Substantial amounts of TL-conjugates remained bound to the intestinal epithelium, or at least were retained within the mucus for several hours in spite of gut peristalsis and mucus sloughing, factors that usually prevent non-specific adherence. Fifteen percent of the dose adhering to the intestinal epithelium most probably derives from the final dose administered 24h earlier. Figure 2A shows the accumulation of nanoparticles within the mucus layer, possibly a prelude to absorption. As the mucus layer is several micrometers thick the penetration of nanoparticles through this gel would appear to be the main barrier for oral particulate absorption. However non-motile bacteria such as *Shigella flexneri* are able to penetrate the mucus layer to invade the lamina propria, this being attributed to the movement of the organism along the natural lines of stress of the moving mucus(17). Figure 2B demonstrates the passage of TL-nanoparticles along the serosal layer, indicative of true absorption.

Low uptake in organised lymphoid tissue (Peyer's patches) is probably related to the reduced availability of specific sugar residues complementary to the TL binding sites over the M-cell apical membrane compared to the enterocytes, although this has to be confirmed histologically. Also, the most abundant cell in the intestine is the enterocyte, compared to the M-cells which constitute less than 1% of the intestinal epithelial cell population. Figure 2C shows the absence of TL-conjugated nanoparticles in the Peyer's patch domes in contrast to blocked nanoparticles which are intimately associated with the blind-

ended lymphatics (figure 2D) demonstrating the re-direction of particles bearing lectins through the villous tissue.

Systemic Appearance of Intestinal Absorbed Nanoparticles

It is evident from Table 1 (and Figure 2E) that after epithelial internalization of TL-conjugated nanoparticles, they are able to traverse the enterocyte basement membrane, enter the lymphatics in the submucosa and translocate to various organs once the lymph drains into the right sub-clavian vein. The spleen and blood (2mL sample) show the greatest uptake on the basis of organ weight but if the blood value is extrapolated to include the whole blood volume of a rat (12 mL for 190 g rats) (18), the accumulation after 5 days rises to 18% giving a total systemic uptake of 23%, an almost 50 fold increase in uptake compared to the uptake of blocked nanoparticles (<0.5%). In contrast the systemic appearance of blocked nanoparticles is limited to the spleen; no nanoparticles could be detected in the liver. Presumably, this is due to the fact that blocked nanoparticles do not bind to the intestinal epithelium that is obviously a prerequisite step for the appearance of particles in the systemic circulation. Figure 2F demonstrates the low accumulation of nanoparticles in the centrilobular vein of the lobuli hepatis amongst the dehydrated erythrocytes. Splenic uptake is higher on the basis of organ weight due to its slow percolating microcirculation and parenchyma rich in lymphatic tissue. The low amount of latex in the heart and kidneys is probably due to the retention of TL-nanoparticles in the coagulated blood of the capillaries upon sacrifice.

DISCUSSION

Several authors have discussed the possibility of targeting Peyer's patches by optimising carrier nanoparticle surface characteristics such as hydrophobicity (19–20). There is some presumption that the degree of accumulation of nanoparticles is directly proportional to their surface hydrophobicity, however Wils *et al.* (21) have shown that extremes of lipophilicity of drugs may lead to decreased transepithelial permeability. A similar situation may also exist for nanoparticles. The effect of

Table 1. Oral Uptake of Tomato Lectin-Conjugated (TL) and Blocked Nanoparticles (500 nm) as a Function of Total Dose Administered and Organ Weight^a

Tissue	TL Nanoparticles		TL nanoparticles with N-acetylchitotetraose	
	(%)	(%/g tissue)	(%)	(%/g tissue)
Intestine	12.8 ± 3.00	4.82 ± 2.10	n/d	n/d
Peyer's patches	0.89 ± 0.04	2.16 ± 1.21	n/d	n/d
Colon	0.90 ± 0.02	0.75 ± 0.01	1.11 ± 0.68	1.10 ± 0.67
Liver	2.64 ± 1.70	0.43 ± 0.28	n/d	n/d
Spleen	1.17 ± 0.80	2.88 ± 1.45	0.42 ± 0.38	0.74 ± 0.67
Blood ^b	3.04 ± 0.64	1.82 ± 0.04	n/d	n/d
Heart	0.29 ± 0.03	0.45 ± 0.06	n/d	n/d
Kidney	0.67 ± 0.16	0.48 ± 0.20	n/d	n/d
Systemic ^c	23.0 ± 6.53		0.42 ± 0.38	

^a Errors presented as standard deviations; n = 4; n/d = not detectable.

^b 2.0 mL blood sample used taken directly through the heart.

^c Extrapolation to whole blood volume (12 mL for 200 g rat).

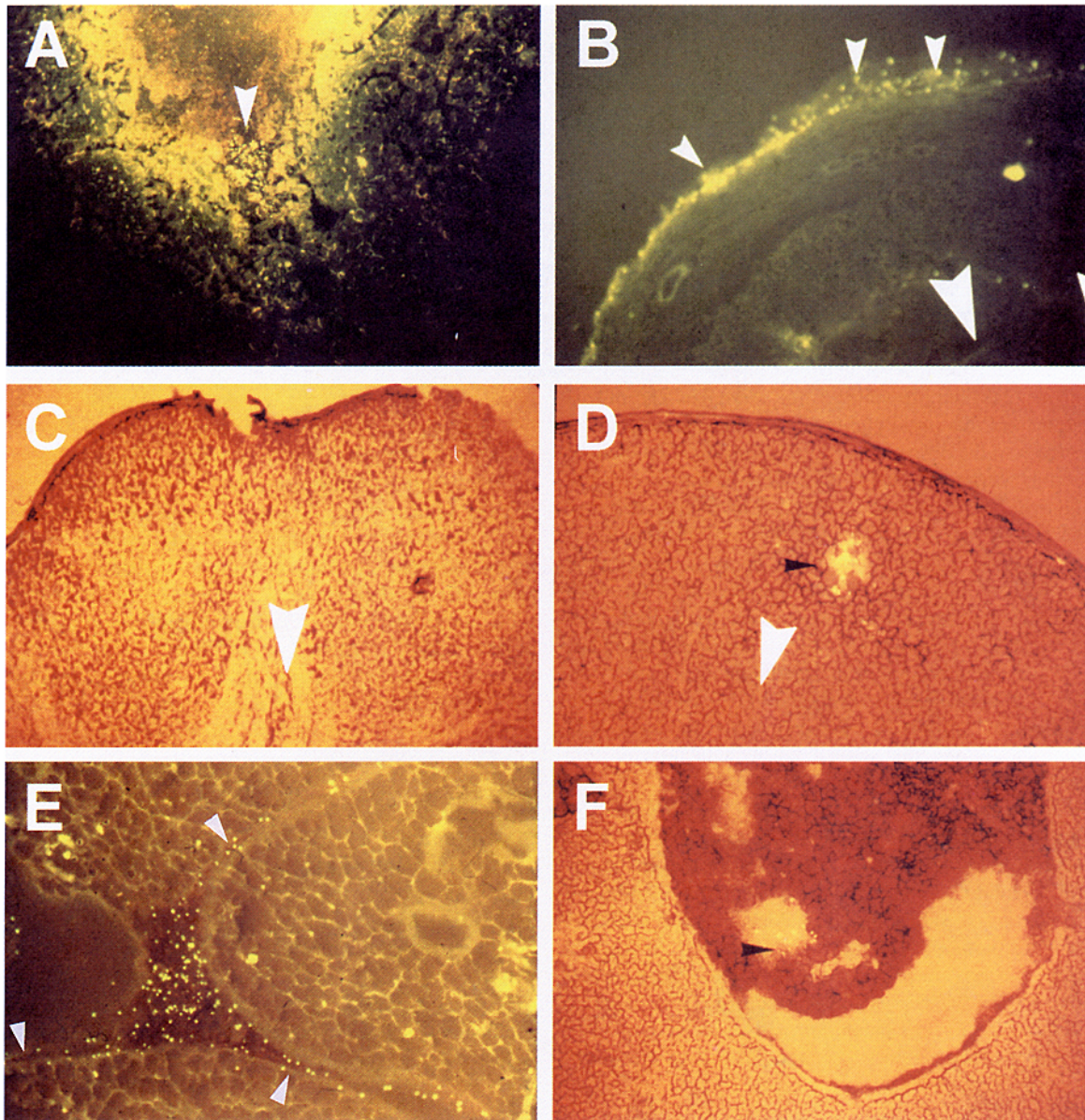


Fig. 2(A-F). In all photomicrographs of the intestine, a large white arrowhead denotes the direction of the intestinal lumen. Smaller arrowheads (either black or white for clarity depending on the background colour) are used to show the anatomical location of the nanoparticles. (A) Photomicrograph ($\times 30$) showing the accumulation of lectin-conjugated nanoparticles between villous tissue amongst the adherent mucus layer, a prelude to absorption. (B) Photomicrograph ($\times 60$) demonstrating the movement of lectin-conjugated nanoparticles across two distinct histological layers, the submucosa and the serosal layer, in a cylindrical section of non-Peyer's patch tissue. (C) Photomicrograph ($\times 40$) from a section of Peyer's patch demonstrating the absence of lectin-conjugated nanoparticles in the dome region. (D) Photomicrograph ($\times 45$) of blocked nanoparticles showing intimate association with lymphatics in the follicle region of the Peyer's patch, a prelude to systemic absorption via the mesentery nodes. Lectin-conjugated nanoparticles in contrast are absent from this region (figure 4) due possibly to the lack of complementary glycoconjugates on the overlying glycocalyx which are probably more abundant over villous tissue compared to Peyer's patch, thus reducing absorption from this route. (E) Concentrated areas of nanoparticles are clearly visible at the junction of three medullary cords of a mesentery node. The nanoparticles travel along distinct pathways of the reticular fibres as shown by the arrowheads converging into a central hollow suggesting that the route of intestinally absorbed nanoparticles to the systemic circulation is via the villous lacteals, which have incomplete basement membranes and wider fenestrations, rather than villous blood capillaries ($\times 80$). (F) Clusters of lectin-conjugated nanoparticles accumulated in the centrilobular vein of lobuli hepatis of a liver hepatocyte amongst the dehydrated erythrocytes, indicative of true systemic translocation of orally administered 500 nm particles ($\times 30$).

particle charge on the magnitude of absorption remains debatable, previous work in this laboratory finding considerable reduction in absorption of negatively charged particles compared with non-ionised polystyrene (22) although uptake of negatively charged liposomes particularly through the Peyer's patches has recently been demonstrated (23).

One approach to overcome non-specificity of interaction is to exploit a receptor mediated process within the GIT such as the vitamin B12 receptor (24), endogenous integral membrane lectins (25) and alpha-beta integrin (invasin) receptors exploited by certain bacteria (26–27). In recent years several approaches along these lines have been tried with modest success but all suffer from inherent disadvantages. In an elegant study Pappo and Ermak (28) demonstrated that latex nanoparticles displaying surface adsorbed anti-M-cell antibody 5B11 (IgM) adhered to and were absorbed by rabbit M-cells three times more efficiently than particles displaying IgM of an unrelated specificity or particles displaying their native surface chemistry. The sigma (s1) outer protein of Reovirus 1, which binds specifically to Peyer's patches, when incorporated in liposomes resulted in a 20 fold uptake through the Peyer's patches compared to villous tissue but the possibility of an intestinal sIgA antibody response generated against these ligands cannot be ruled out after repeated administration (29).

Although recent evidence suggests that Peyer's patches are the major sites of colloidal uptake via specialised M-cells (8) the present study reveals a 14-fold increase in the adsorption/absorption of TL-nanoparticles through the non-lymphoid villous epithelium. The mapping of lectin binding sites over the rat M-cells and enterocytes by Owen and Bhalla (30) showed the equal binding of 3 different lectins, including wheat germ agglutinin which has a similar binding specificity to TL (via poly-N-acetylglucosamine residues). Given the assumption that the density of TL-binding structures on villous and lymphoid tissue is similar, then preferential uptake of TL-binding structures on villous and lymphoid tissue is similar, then preferential uptake of TL-conjugated nanoparticles via the villous tissue is a function of the surface area available. Reduced TL-binding sites over the follicle-associated epithelium thus probably directs intestinal absorption of nanoparticles through the non-lymphoid tissue. Site-specific delivery of agents to Peyer's patches with lectins is compromised by the lack of data concerning the mapping of lectin-binding structures that have not revealed carbohydrate sites unique to the M-cell surface of rat Peyer's patches. This is in contrast to mouse and rabbit M-cells (31). The situation is further complicated by recent findings that specific-lectin binding to Peyer's patches is dependent upon the anatomical location of gut lymphoid tissue within the same species (31).

According to Walker (32) the preferred route of uptake of low concentrations of luminal antigens is through the M-cells, but at higher concentrations the enterocytes are also involved. Furthermore Sternson (33) pointed out that Peyer's patches uptake is compromised by the limited efficiency and capacity of the pathway. Pappo and Ermak (34) confirmed Sternson's hypothesis showing that only 5% of the total dose of 500 nm latex particles placed in rabbit ligated loops containing Peyer's patches were taken up in a single round of endocytosis and no additional nanoparticles adhered to the M-cell membrane during the next 90 min. Porta *et al.* (35) further showed that <3% of M-cells could both adhere and internalize particles and that

only half of the mouse M-cell population had endocytic capability. This indicates, in line with our results, that the importance attached to the Peyer's patches as the principal site of particulate absorption may have been over-emphasised, and that normal epithelial cells can also be induced, with appropriate ligands such as plant lectins and bacterial adhesins, to absorb particulate matter.

The high circulating levels of nanoparticles in the blood indicates both true intestinal absorption and the inability of the reticuloendothelial system to sequester them, due perhaps to remnants of TL still present on the nanoparticles or the negatively charged carboxyl groups which may act like bacterial capsular polysaccharides in exhibiting anti-phagocytic activity. This appears to be the first time that orally applied nanoparticles are shown to avoid hepatic capture.

Although numerous investigators have suggested the use of TL as a bioadhesive component of drug delivery systems the *in vivo* data in this paper represents the first full test of the consequences of the incorporation of this lectin on to a delivery system. Furthermore our data indicates not only the permeability of the conjugates through the mucus but the absence of significant impedance of intestinal uptake due to lectin interaction with mucus (11). In addition it is seen that TL allows the internalization of the nanoparticles through the villous tissue, probably due to the ubiquitous presence of N-acetylglucosamine residues on the epithelial surface of the gastrointestinal tract. Since the non-lymphoid intestinal epithelium comprises a greater surface area compared to M-cells, the use of bioadhesive ligands, which possess complementary intestinal binding sites in large numbers, offers a vast area of uptake of colloidal particles, not now restricted to Peyer's patches.

Several questions of course remain unanswered. The effect of interaction of the particles and lectins with food and commensal gut flora and any subsequent effect on local gut ecology is not known. However the *in vivo* data presented here gives further impetus to the possibility for the use of TL-like molecules in oral delivery systems.

ACKNOWLEDGMENTS

Nasir Hussain was supported by a joint Royal Pharmaceutical Society of Great Britain and Syntex Research Centre CRISP award and the late Dr P.U. Jani by a Maplethorpe Fellowship of the University of London. We are grateful to Mr David McCarthy for the histology and preparation of photographs. We also thank Prof. Calum B. Macfarlane and Dr John Langridge, formerly of Syntex Research, Edinburgh for their support and advice in the project. We would also like to extend our thanks to Biomedical Communications/Arts Department of St Jude Children's Research Hospital for their additional meticulous work on the photomicrographs.

REFERENCES

1. A. T. Florence and P. U. Jani. In A. Rolland (ed.), *Pharmaceutical Particulate Carriers: Therapeutic Applications.*, Marcel Dekker, New York, 1993, pp. 65–107.
2. P. U. Jani, G. W. Halbert, J. Langridge, and A. T. Florence. *J. Pharm. Pharmacol.* **42**:821–826 (1990).
3. P. U. Jani, A. T. Florence, and D. E. McCarthy. *Int. J. Pharm.* **84**:245–252 (1992).
4. E. Sanders and C. T. Ashworth. *Exp. Cell. Res.* **22**:137–145 (1961).

5. D. D. Joel, J. A. Laissue, and M. E. LeFevre. *J. Reticuloendothel. Soc.* **24**:477-487 (1978).
6. J. S. Trier. *Gastroenterol. Clinics. North Amer.* **20**:531-547 (1990).
7. D. E. Bockmann and M. D. Cooper. *Am. J. Anat.* **136**:455-477 (1973).
8. W. Sass, H. P. Dreyer, and J. Seifert. *Am. J. Gastroenterol.* **85**:255-260 (1990).
9. A. Pustzai. *Adv. Drug Deliv. Rev.* **3**:215-228 (1989).
10. B. Naisbett and J. F. Woodley. *Biochem. Soc. Trans.* **17**:883 (1989).
11. C. M. Lehr, J. A. Bouwstra, W. Kok, A. B. J. Noach, A. G. de Boer, and H. E. Junginger. *Pharm. Res.* **9**:547-553 (1992).
12. N. Hussain, P. U. Jani and A. T. Florence. *Proc. Soc. Control. Rel. Bioact. Mat.* **21**:115 (1994).
13. D. C. Kilpatrick, A. Pustzai, and G. Grant. *FEBS Lett.* **185**:299-305 (1985).
14. M. S. Nachbar, J. D. Oppenheim, and J. O. Thomas. *J. Biol. Chem.* **255**:2056-2061 (1980).
15. J. M. Irache, C. Durrer, D. Duchêne and G. Ponchel. *Biomaterials* **15**:899-904 (1994).
16. T. Basinka and S. Slomokowsk. *Biomater. Sci. Polym.* **3**:115-125 (1991).
17. R. Freter. In J. Roth (ed.), *Virulence Mechanisms of Bacterial Pathogens*. American Society for Microbiology, New York, 1988, pp. 45-60.
18. H. J. Baker, R. J. Lindsey, and S. H. Weisbroth. *The Laboratory Rat*. Academic Press, New York, 1979.
19. M. A. Jepson, L. N. Simmons, T. D. O'Hagan, and B. H. Hirst. *J. Drug Target.* **1**:1-15 (1993).
20. J. H. Eldridge, C. J. Hammond, J. A. Meulbroek, J. K. Staas, R. M. Gilley, and T. R. Tice. *J. Control. Rel.* **1**:205-214 (1990).
21. P. Wils, A. Warnery, V. Phung-Ba, S. Legrain, and D. Scherman. *J. Pharmacol. Exp. Therap.* **2**:654-658 (1994).
22. P. U. Jani, G. W. Halbert, J. Langridge, A. T. Florence. *J. Pharm. Pharmacol.* **41**:809-812 (1989).
23. H. Tomizawa, Y. Aramaki, Y. Fujii, T. Hara, N. Suzuki, K. Yachi, H. Kikuchi, and S. Tsuchiya. *Pharm. Res.* **10**:549-552 (1993).
24. G. J. Russell-Jones, H. J. De Azipurua. *Proc. Inter. Symp. Control Rel. Bioact. Mater.* **15**:142-143 (1988).
25. B. Říhová, C. R. Rathi, P. Kopecková, and J. Kopecek. *Int. J. Pharm.* **87**:105-116 (1992).
26. G. Tran van Nhieu and R. R. Isberg. *Ann. Rev. Genet.* **27**:395-422 (1994).
27. N. Hussain and A. T. Florence. *J. Control. Rel.* **41**:S3-4 (1996).
28. J. Pappo, T. H. Ermak, and H. J. Stieger. *Immunology* **73**:277-280 (1991).
29. W. Rubas, A. C. Banerjea, H. Gallati, P. P. Spieger, and W. K. Jokilk. *J. Microencap.* **7**:385-395 (1990).
30. R. L. Owen and D. K. Bhalla. *Am. J. Anat.* **168**:199-212 (1983).
31. M. A. Jepson, C. M. Mason, and M. A. Clark. *J. Drug Target.* **3**:75-77 (1995).
32. W. A. Walker and I. R. Sanderson. *Ann. N. Y. Acad. Sci.* **664**:7-10 (1992).
33. L. A. Sternson. Obstacles to polypeptide delivery. *Ann. N. Y. Acad. Sci.* **507**:19-22 (1987).
34. J. Pappo, and T. H. Ermak. *Clin. Exp. Immunol.* **76**:144-148 (1989).
35. C. Porta, P. S. James, A. D. Phillips, T. C. Savidge, M. W. Smith, and D. Cremaschi. *Exp. Phys.* **77**:929-932 (1992).